Nonlinear-optic and ferroelectric behavior of lithium borate–strontium bismuth tantalate glass–ceramic composite

G. Senthil Murugan and K. B. R. Varma[a)]
Materials Research Centre, Indian Institute of Science, Bangalore-560012, India

Yoshihiro Takahashi and Takayuki Komatsu
Department of Chemistry, Nagaoka University of Technology, Nagaoka 940-2188, India

Transparent glasses in the system (100–x) $Li_2B_4O_7$–$x$$SrBi_2Ta_2O_9$ ($0 \leqslant x \leqslant 20$) were fabricated via a splat-quenching technique. The glassy nature of the as-quenched samples was established by differential thermal analyses. X-ray powder diffraction and transmission electron microscopic studies confirmed the amorphous nature of the as-quenched and crystallinity (40 nm) in the heat-treated (glass–ceramic) samples. The dielectric constant (ϵ_r) of the glass–ceramic composite ($x=20$, heat treated at 773 K/8 h) was in between that of the parent host glass ($Li_2B_4O_7$) and strontium bismuth tantalate ceramics in the frequency range 100 Hz–40 MHz at 300 K. These exhibited intense second-harmonic generation and a ferroelectric hysteritic behavior (P vs E loops) at 300 K. The coercive field (E_c) and the remnant polarization (P_r) were 1053 V/cm and 0.483 μC/cm^2, respectively.

Transparent polar glass ceramics comprising nano/microcrystallites that are capable of exhibiting piezo-, pyro-, ferroelectric, and nonlinear optical (NLO) properties have been in increasing demand and recognized to be potential multifunctional materials. Among a variety of polar glass ceramics that were investigated for various physical properties, tellurium dioxide (TeO_2)-based glasses were promising for use in nonlinear optical devices because of their refractive-index compatibility with those of well-known ferroelectric compounds.[1,2] Apart from this, these glasses were known to exhibit large third-order nonlinear optical effects.[3] We have recently examined the possibility of growing ferroelectric crystals belonging to the Aurivillius family of layered ferroelectric oxides of the homologous series $[Bi_2O_2]^{2+}[A_{n-1}B_nO_{3n+1}]^{2-}$, in strontium borate and lithium borate glass matrices[4,5] for possible applications in pyro- and ferroelectric-based devices. In the present letter, we report the nanocrystallization of strontium bismuth tantalate ($n=2$ member of the homologous series) in a lithium borate glass matrix. The dielectric, ferroelectric, and nonlinear optical properties of the composite of different compositions [(100–x) $Li_2B_4O_7$–x $SrBi_2Ta_2O_9$, x ranging from 0 to 20 in molar ratio] heat treated at 773 K for 8 h are also elucidated.

Transparent glasses of optical quality in the nominal composition (100–x) $Li_2B_4O_7$–x $SrBi_2Ta_2O_9$ (x ranging from 0 to 20, in molar ratio) were fabricated via a conventional splat-quenching technique. The polycrystalline compounds $Li_2B_4O_7$ (LBO) and $SrBi_2Ta_2O_9$ (SBT) that were used for the present studies were prepared from their respective oxides (B_2O_3, Bi_2O_3, Ta_2O_5) and carbonates (Li_2CO_3 and $SrCO_3$) by the conventional solid-state reaction route. LBO and SBT in different molar ratios were ground well in a mortar and pestle in an acetone medium for an hour and transferred to a platinum crucible. The platinum crucible containing the mixture covered with a lid was placed in a melt-quenching programmable furnace (Lenton), the temperature was raised to 1375 K (the heating rate used was 5 K/min), and maintained at that temperature for 30 min. Subsequently, the melt was poured on to a preheated (400 K) stainless-steel plate and quickly pressed by another stainless-steel plate. The flat glass plates (dimensions: 20–25 mm diam, 1–2 mm thickness), thus obtained, were annealed at 475 K for 6 h (the heating and cooling rates were 50 K/h) to relieve them of thermal stresses.

Differential thermal analysis (DTA) (STA 1500, Polymer Laboratory) was employed to ascertain the glassy nature of the as-quenched samples and to find out the glass transition (T_g), crystallization (T_{cr}), and melting (T_m) temperatures. The heating rate maintained for this purpose was 15 K/min. The crushed powders of different compositions of the as-quenched glass and the glass–ceramic composite plates were subjected to x-ray powder diffraction (XRD) (Scintag) to confirm their respective amorphous and crystalline natures. Structural details of the as-quenched and the glass–ceramic composite samples were corroborated using transmission electron microscopic (TEM) (JEOL-JEM 200CX) and selected area electron diffraction (SAD) studies.

Capacitance and dielectric loss (D) measurements were performed on the glass and glass–ceramic composites using an impedance gain phase analyzer (HP 4194A) in the frequency range 100 Hz–40 MHz at different temperatures. For these measurements, gold was sputtered on both surfaces of the samples and copper leads were bonded to them with silver epoxy. The ferroelectric hysteresis loop (P vs E) was recorded at a switching frequency of 50 Hz with a modified Sawyer–Tower circuit[6] associated with an adjustable RC compensation circuit. The values of remnant polarization (P_r) and the coercive field (E_c) were determined from the hysteresis loop at 300 K. The second-harmonic (SH) inten-

[a)]Author to whom correspondence should be addressed; electronic mail: kbrvarma@mrc.iisc.ernet.in

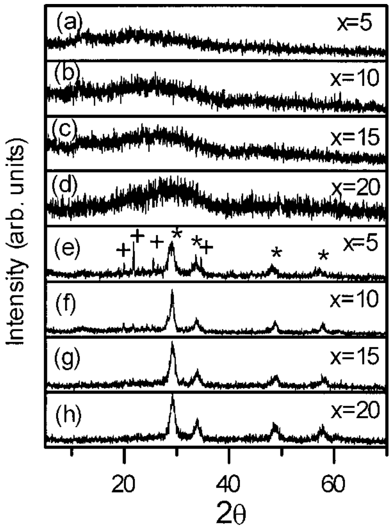

FIG. 1. XRD patterns [(a)–(d)] for the as-quenched and [(e)–(h)] for the sample heat treated at 773 K/8 h (+ LBO phase and * SBT phase).

sity (532 nm) of the glass ceramic composites of different compositions has been measured at 300 K using the fundamental wave of a pulsed Nd:YAG laser via the Maker fringe method.[7] The second-harmonic intensity was observed in *p*-excitation and *p*-detection mode.

The XRD patterns obtained for all the compositions of the as-quenched samples ($0 \leqslant x \leqslant 20$) were confirmed to be amorphous and are depicted in Figs. 1(a)–1(d) for their representative compositions. The DTA traces that were recorded for the samples corresponding to the composition ranging from 5 to 20 mol % [Figs. 2(a)–2(d)] establish their glassy nature. These plots show endotherms (glass transition temperature T_g) in the temperature range 730–750 K, depending on the extent of x. The exotherms corresponding to the crystallization temperatures (T_{cr1} and T_{cr2}) were found to occur in the range 790–880 K. A subsequent endotherm that is encountered around 1150 K is attributed to the melting of the

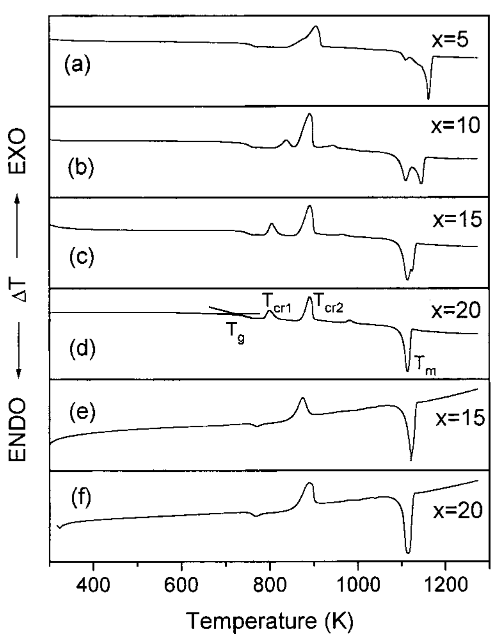

FIG. 2. Differential thermograms of the as-quenched and heat-treated LBO–SBT composite samples of various compositions.

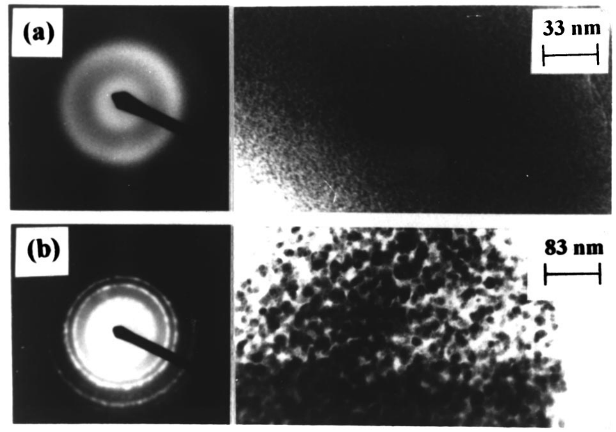

FIG. 3. Transmission electron micrographs of (a) the as-quenched sample and (b) the sample heat-treated at 773 K for 8 h, with corresponding electron diffraction patterns for the composition $x = 20$.

glass composite. The XRD patterns of the samples of different compositions heat treated isothermally at 773 K for 8 h, which is close to the onset of the first exotherm (T_{cr1}), are shown in Figs. 1(e)–1(h). Interestingly, the glass–ceramic composites for $10 < x \leqslant 20$ are transparent and the XRD depicts only the presence of monophasic crystalline SBT. On the other hand, the glass ceramic composites for $x \leqslant 10$ are translucent and the XRD shows the presence of LBO crystalline peaks in addition to that of SBT. It implies that higher (>10 mol %) concentrations of SBT prevent the crystallization of LBO glass. Further, it is confirmed based on XRD studies that the LBO crystallization is confined only to the surface of the sample while that of SBT was found to be a bulk process. The XRD patterns obtained for unpolished flat plates showed peaks corresponding to the LBO crystalline phase along with that of SBT. The same samples when subjected to XRD studies subsequent to the removal of a few surface layers (to the extent of a few micrometers) did not reveal the presence of LBO peaks. The SBT crystallite size in the LBO matrix for the $x = 20$ glass–ceramic composite is found to be around 40 nm by the x-ray line-broadening method.[8]

Figure 3 shows the transmission electron micrographs along with the selected area electron diffraction patterns of the as-quenched [Fig. 3(a)] and glass–ceramic composite [Fig. 3(b)] for the representative composition $x = 20$. The SAD pattern [Fig. 3(a)] confirms its amorphous nature. However, the presence of broad spherical rings around the central bright region reveals the existence of fine crystallites in the glassy matrix which is evidenced from the respective micrograph. The micrograph in Fig. 3(b) reveals the presence of nearly spherical crystallites that are more or less uniformly dispersed in the LBO glass matrix. The average crystallite size, estimated based on electron microscopic analyses, is around 30 nm ($x = 20$), which is less than that obtained by XRD studies and is possibly due to the experimental limitation that is involved in XRD studies. The SAD pattern in Fig. 3(b) confirms the crystalline nature of the glass–ceramic composite. The d spacings and the lattice parameters that are computed based on the SAD pattern are found to compare well with that of SBT reported in the literature.[9]

The dielectric constant of the glass–ceramic composite

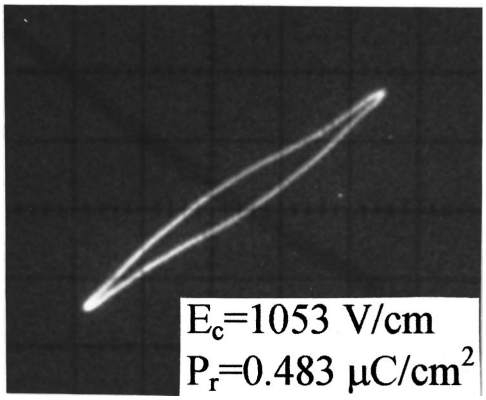

FIG. 4. Ferroelectric hysteresis loop for the LBO–SBT glass–ceramic composite corresponding to the composition $x=15$.

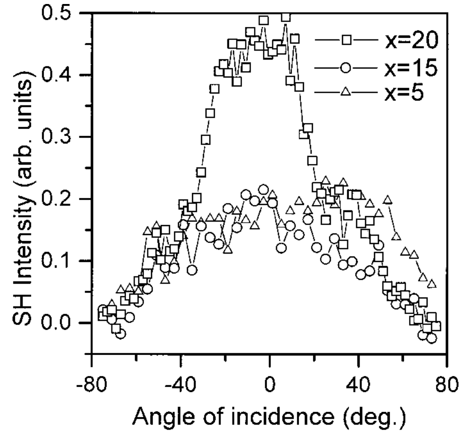

FIG. 5. Second–harmonic intensities (532 nm) for the glass–ceramic composites of three compositions as a function of the incident angle of the laser (1064 nm).

$(5 \leqslant x \leqslant 20)$ increases and the dielectric loss decreases steadily with increase in x. It is remarkable to note that the dielectric loss of the glass–ceramic composites is less (0.035 at 100 kHz for $x=20$) by an order of magnitude than that of the parent lithium borate glass and strontium bismuth tantalate ceramic at 300 K. Typical values of D for lithium borate glass and polycrystalline strontium bismuth tantalate reported in the literature were 0.2 and 0.22 (at 100 kHz).[10,11] Also, it is interesting to note that as the composition of SBT in LBO increases, the dielectric loss decreases, which is an important feature to be considered, particularly for pyro- and ferroelectric device applications. The dielectric constant and dielectric loss decrease with increase in frequency. The dispersion in ϵ_r and D with frequency is significant until about 10 kHz and, subsequently, the dispersion is very small until the maximum frequency (40 MHz) covered in the present investigations. The Cole–Cole plot generated between the real (Z') and imaginary part (Z'') of the impedance shows a depressed semicircle with its center lying below the x axis, confirming the relaxation involved to be non-Debye type. The ferroelectric properties of the present glass–ceramic composite are interesting. The ferroelectric hysteresis (P vs E) loop for the glass-ceramic composite of the representative composition corresponding to $x=15$ recorded at room temperature is shown in Fig. 4. This loop is reminiscent of the ferroelectric nature of the layered ferroelectric oxides. The P_r and E_c values at 300 K for the $x=15$ glass–ceramic composite are 0.483 μC/cm^2 and 1053 V/cm. The P_r values of the present composites are much less than that obtained for both bulk and thin films of pure SBT.

The glass–ceramic composites ($x>10$) containing nanocrystalline ferroelectric $SrBi_2Ta_2O_9$ were optically transparent, which enabled us to measure the second-harmonic generation (SHG) (532 nm). We show the variation of SH intensity with the incident angle of the laser for the glass–ceramic composites in Fig. 5. The pronounced second-harmonic signals are observed in the samples corresponding to the compositions $x=5$, 15, and 20 mol %. Particularly, the SHG intensity for the sample with $x=20$ is higher than those for the other samples. It was also found that the SHG intensity increases with increasing poling field and heat-treatment temperature in the range 723–773 K. The details of which will be communicated shortly.

In summary, a lithium borate and strontium bismuth tantalate glass–ceramic composites were proved to be a potential candidate for nonlinear optical applications. The most interesting aspect of the present investigations has been the observation of ferroelectric hysteritic behavior associated with low dielectric loss at 300 K in glass–ceramic composites containing 40-nm-sized crystallites of SBT.

This work was financially supported from the Council of Scientific and Industrial Research (CSIR), Government of India.

[1] K. Shioya, T. Komatsu, H. G. Kim, R. Sato, and K. Matusita, J. Non-Cryst. Solids **189**, 16 (1995).
[2] H. G. Kim, T. Komatsu, K. Shioya, K. Matusita, K. Tanaka, and K. Hirao, J. Non-Cryst. Solids **208**, 303 (1996).
[3] S. H. Kim, T. Yoko, and S. Sakka, J. Am. Ceram. Soc. **76**, 2486 (1993).
[4] M. V. Shankar and K. B. R. Varma, J. Non-Cryst. Solids **226**, 145 (1998).
[5] G. Senthil Murugan and K. B. R. Varma, Mater. Res. Bull. **34**, 2201 (1999).
[6] C. B. Sawyer and C. H. Tower, Phys. Rev. **35**, 269 (1930).
[7] P. D. Maker, R. W. Terhune, M. Nisenoff, and C. M. Savage, Phys. Rev. Lett. **8**, 21 (1962).
[8] H. P. Clug and L. E. Alexander, *X-Ray Diffraction Procedures* (Wiley, New York, 1974), p. 643.
[9] A. D. Rae, J. G. Thompson, and R. L. Withers, Acta Crystallogr., Sect. B: Struct. Sci. **B48**, 418 (1992).
[10] G. Senthil Murugan, G. N. Subbanna, and K. B. R. Varma, Ferroelectr. Lett. Sect. **26**, 1 (1999).
[11] J. S. Yang and X. M. Chen, Mater. Lett. **29**, 73 (1996).